Impact of vegetation types on surface temperature change

Young-Kwon Lim

Center for Ocean-Atmospheric Prediction Studies (COAPS),

Florida State University, Tallahassee, FL 32306-2840

Ming Cai

Department of Meteorology,

Florida State University, Tallahassee, FL 32306-4520

Eugenia Kalnay

Department of Atmospheric and Oceanic Science,

University of Maryland, College Park, MD 20742-2425

and

Liming Zhou

School of Earth and Atmospheric Sciences,

Georgia Institute of Technology, Atlanta, GA 30332-0340

Revision Submitted to Journal of Applied Meteorology and Climatology

January 29, 2007

Abstract

The impact of different surface vegetations on long-term surface temperature change is estimated by subtracting reanalysis trends in monthly surface temperature anomalies from observation trends over the last four decades. This is done using two reanalyses, namely, ECMWF-40 (ERA40) and NCEP-NCAR I (NNR), and two observation datasets, namely, Climatic Research Unit (CRU) and Global Historical Climate Network (GHCN). The basis of the observation minus reanalysis (OMR) approach is that the NNR reanalysis surface fields, and to a lesser extent the ERA40, are insensitive to surface processes associated with different vegetation types and their changes because the NNR does not use surface observations over land, whereas ERA40 only uses surface temperature observations indirectly, in order to initialize soil temperature and moisture. As a result, the OMR trends can provide an estimate of surface effects on the observed temperature trends missing in the reanalyses.

The OMR trends obtained from observation minus NNR show a strong and coherent sensitivity to the independently estimated surface vegetation from Normalized Difference Vegetation Index (NDVI). The correlation between the OMR trend and the NDVI indicates that the OMR trend decreases with surface vegetation, with a correlation < -0.5, indicating that there is a stronger surface response to global warming in arid regions, whereas the OMR response is reduced in highly vegetated areas. The OMR trend averaged over the desert areas ($0 <$ NDVI < 0.1) shows a much larger increase of temperature (~0.4°C/decade) than over tropical forest areas (NDVI > 0.4) where the OMR trend is nearly zero.

Areas of intermediate vegetation (0.1 < NDVI < 0.4), which are mostly found over mid-latitudes, reveal moderate OMR trends (0.1~0.3°C/decade).

The OMR trends are also very sensitive to the seasonal vegetation change. While the OMR trends have little seasonal dependence over deserts and tropical forests, whose vegetation state remains rather constant throughout the year, the OMR trends over the mid-latitudes, in particular Europe and North America, exhibit strong seasonal variation in response to the NDVI fluctuations associated with deciduous vegetation. The OMR trend rises up to 0.2~0.3°C/decade in winter and early spring when the vegetation cover is low, and is only 0.1°C/decade in summer and early fall with high vegetation. However, the Asian inlands (Russia, northern China with Tibet, and Mongolia) do not show this strong OMR variation despite of their mid-latitude location, due to the relatively permanent aridity of these regions.

1. Introduction

Global mean surface temperature time series derived from in-situ observations reveal the inter-decadal global warming over the last several decades (IPCC 2001). Many studies reported that this upward trend is significantly a result of primary human impacts such as greenhouse gases (IPCC 2001) and land use (Pielke et al. 2002). The anthropogenic land use impact on surface warming may become more important as the surface vegetation changes in the form of urbanization, agricultural activity, and deforestation.

The impact of surface temperature changes forced by different regional vegetation types is not well documented. Only urban impact has been assessed by comparing observations in cities with those in rural areas (Easterling et al. 1996; Hansen et al. 2001). But this approach is only applicable to urban effects, and the estimated signals vary with the criteria in classifying urban and rural areas.

The present study is motivated by the difficulty in separating the surface temperature change signals due to global and regional forcings in the observed data. The basis of this study is the fact that the surface temperature change response to land vegetation types is not present in the NCEP/NCAR reanalysis (NNR) surface data, and is only partially present in the ECMWF 40-year reanalysis (ERA40), while the station data include not only local surface forcings but the large-scale atmospheric warming signal resulting from greenhouse effects, natural decadal variability, and volcanoes (Pielke et al. 2002; Kalnay and Cai 2003; Zhou et al. 2004; Frauenfeld et al. 2005; Lim et al. 2005; Kalnay et al. 2006). Impact of the vegetation cover can extend to some extent into the free

atmosphere and thus may influence the atmospheric and surface reanalysis (Kabat et al. 2004), but NNR is substantially insensitive to surface processes associated with different vegetation types because it does not use surface observations over land in the assimilation (Kistler et al. 2001; Kalnay and Cai 2003). Instead, NNR surface temperature fields are estimated from the upper air information combined with model parameterizations of surface processes (Lim et al. 2005) so that the NNR provide a dynamically complete dataset of atmospheric variables. ERA40 is somewhat more sensitive to local surface processes than NNR because the surface temperature observations are used in the initialization of soil temperature and moisture (Simmons et al. 2004).

Evaluation of reanalyzed tropical temperature time series archived from ERA40 (Palmer et al. 1990; Betts et al. 2003; Simmons et al. 2004) and NNR (Kalnay et al. 1996; Kistler et al. 2001) indicate that the climatic trend derived from reanalysis data capture the upward surface temperature trends but that the trend is not identical to that of observed data (Chelliah and Ropelewski 2000; Hegerl and Wallace 2002; Kalnay and Cai 2003; Simmons et al. 2004; Lim et al. 2005; Pepin et al. 2005; Kalnay et al. 2006). Specifically, Simmons et al. (2004) and Lim et al. (2005) reported that the hemispheric average in two reanalyses (ERA40 and NNR) have a smaller warming trend than that of observations. They suggest that this smaller trend arises from the fact that the reanalysis data do not adequately reproduce the long-term surface climatic trend driven by the impact of independent land-cover types.

These characteristics of the reanalysis provide us with the possibility of

detecting surface temperature change signals due to regional land vegetation types by taking the difference between observed and reanalysis temperature time series (Observation minus Reanalysis (OMR)). The present study, therefore, has as objectives 1) to find the relationship between OMR trend and the regional land vegetation types in terms of surface vegetation index and 2) to estimate the temperature change signal as a function of surface vegetation indexes.

It has been argued that errors such as reanalysis inhomogeneity in time, model systematic errors, including the lack of trends in the greenhouse gases, and observation biases could contaminate the true surface temperature change signal (Trenberth 2004; Vose et al. 2004; Cai and Kalnay 2004). Cai and Kalnay (2005) showed analytically that a reanalysis made with a model without anthropogenic forcing could capture the observed trends if they are present in the observations assimilated. Our OMR analysis tries to minimize the impact of those errors by 1) averaging for the relatively homogeneous reanalysis period, 2) computing the trend of the anomalies with respect to the annual cycle, and 3) choosing the most reliable observation data currently available.

There have been several studies using OMR trends for estimating of the regional surface warming signal driven by different land vegetation types. Kalnay and Cai (2003) assessed the decadal surface warming trend associated with regional land uses over the eastern U.S. by subtracting reanalysis trend from observed one. Kalnay et al. (2006) found regions of OMR warming and cooling, in good agreement with the regional trends obtained by Hansen et al. (2001) when using nightlights to identify rural and urban stations. Zhou et al. (2004),

Frauenfeld (2005), and Lim et al. (2005), using the same method, estimated reasonable values for surface warming trends caused by Chinese urbanization, Tibetan Plateau land uses, and the Northern Hemispheric land vegetation types, respectively. All these authors except Lim et al. (2005) concentrated on regional geographical areas, and are not sufficient to draw an overall conclusion for the globe.

In summary, the advantage of the OMR approach is that the removal of the reanalysis estimates from the surface observations makes possible to isolate the near-surface warming signals associated with the regional surface vegetation types from the warming signals resulting from large-scale atmospheric forcings (e.g., greenhouse gases and volcanoes). As a result, it is expected that the OMR trends can give an estimate of the surface temperature change signal arising from the different types of regional surface vegetation. In the present study, we will attempt to find the relationship between OMR surface warming patterns and land vegetation types in terms of surface vegetation status using Normalized Difference Vegetation Index (NDVI) (Sellers 1985; James and Kalluri 1994) made from satellite-derived greenness values.

Section 2 introduces the observation and the reanalysis temperature data, and the vegetation index data used in this study. Surface temperature time series of observation, reanalysis, and the OMR averaged over major land masses are shown in section 3. Section 4 delineates the geographical distribution of the surface vegetation index, the relationship between OMR trends and the surface vegetation index, and estimates the surface temperature change signal associated with NDVI.

The variation of the OMR in response to the seasonal NDVI change is described in section 5, followed by summary and discussions given in section 6.

2. Data

For this study we use monthly surface temperature from two reanalyses (NNR and ERA40), and from two gridded data sets based on surface observations (Global Historical Climatology Network (GHCN), http://www.ncdc.noaa.gov, Peterson and Vose 1997, and Climatic Research Unit (CRU), http://www.cru.uea.ac.uk, Jones and Moberg 2003), all covering the period 1960-1999. We downloaded observational (GHCN and CRU) data available on a 5°×5° grid. For consistency, the reanalyses data have also been linearly interpolated to the same 5°×5° GHCN and CRU grid.

Since the station coverage declined during the 1990s in the CRU measurements, CRU anomalies were calculated with respect to normals for 1961-1990. For consistency, anomalies of other data have been calculated with respect to their own climatic normals for 1961-1990.

Like the reanalyses, surface observational datasets may also have some limitations, because the observations themselves have some biases. The quality of surface measurement variables tends to depend on the coverage of surface observation network, homogeneity, and the accuracy of surface measurements. In the present study, we use the CRU and GHCN surface temperatures as observed datasets. CRU and GHCN data values are similar, since they draw from over 90% common data, and differ mostly in their processing. Jones and Moberg

(2003) indicate that the gridded (5°×5°) database available on the CRU web site (http://www.cru.uea.ac.uk) comprises 5159 station records, which are more densely distributed over mid-latitudes. The data are also corrected by newly homogenized series with adjustment of the variance of individual grid-box series to remove the effects of changing station numbers through time. As to GHCN (Peterson and Vose 1997), the quality of surface temperature values are enhanced by including a century-scale dataset with monthly surface observations from ~7000 stations from around the world, which make it possible to improve regional-scale analyses, particularly in previously data-sparse areas. Rigorous and objective homogeneity adjustments are performed to decrease the effect of nonclimatic factors on the time series. Therefore, these two observation datasets are accepted as a reliable basis for investigating and assessing surface temperature change signal associated with different vegetation types from the OMR time series. However, we note that both CRU and GHCN have fewer station data per grid point in the tropics than in mid-latitudes, which could reduce the reliability of the gridded observation data in the tropical region.

Normalized Difference Vegetation Index (NDVI) data (Sellers 1985; James and Kalluri 1994), downloaded from http://daac.gsfc.nasa.gov/, are used to find if there is a relationship between the distribution of the surface vegetation and its seasonal changes, and the decadal OMR trends. The NDVI a satellite-derived surface greenness values (Bounoua et al. 2000), is produced using the measurements from the Advanced Very High Resolution Radiometer (AVHRR) on board the NOAA polar orbiting meteorological satellites. The dataset contains the

global monthly composites of the NDVI at 1 degree resolution covering the period from 1981 to 1994. The reflectance measured from channel 1 (visible: 0.58-0.68 μm) and channel 2 (near infrared: 0.725-1.0 μm) are used to calculate the index. The NDVI value is defined as the ratio of the difference to the total reflectance: (channel 2 – channel 1)/(channel 2 + channel 1). Green leaves commonly have larger reflectances in the near infrared than in the visible range. Clouds, water, and snow have larger reflectances in the visible than in the near infrared, so that negative values of the vegetation index may correspond to snow or ice cover, whereas the difference in reflectance is almost zero for bare soils such as deserts. As a result, NDVI values can range from -1.0 to 1.0 but typical ranges are from 0.1 up to 0.7, with higher values associated with greater density and greenness of plant canopies. We have also made comparisons with another NDVI data set derived from GIMMS (Global Inventory Modeling and Mapping Studies) (Tucker et al. 2005) and the results remained similar.

3. Regional surface temperature time series of observation and reanalysis

Surface temperature anomalies averaged over major land regions in the Northern Hemisphere (NH) derived from the two reanalyses and two observations are plotted in Fig. 1. Anomalies are further adjusted to have zero mean over the last 10 years (1993-2002) since the biases of reanalyses are smallest for the most recent years (Simmons et al. 2004). The key features in Fig. 1 are:

(i) The two surface observation datasets (CRU and GHCN) in each panel on the left are nearly indistinguishable (Figs. 1a-d), showing a gradual upward trend of surface

temperature over Asia, Europe, North and South America, and Africa region. The two reanalyses are also in remarkable agreement with the observations in terms of capturing the inter-annual variability and the long-term trends.

(ii) Nevertheless, it is evident that the reanalyses exhibit a smaller warming trend than observations, as reported in Kalnay and Cai (2003) and Lim et al. (2005). This feature is found in all regions (Figs. 1a-d). Because of this, the OMR time series (Figs. 1e-h) obtained by subtracting reanalyses from observations show a positive trend in every region.

(iii) The right panel indicates that overall, the OMR time series with ERA40 yields a smaller warming trend than that derived from the NNR (Figs. 1e-h). This is to be expected because ERA40 uses to some extent the surface observation in their assimilation system, while the NNR does not use the surface information. Land surface temperature and soil moisture in the ERA40 are estimated by assimilating the Climatic Research Unit (CRU) surface observations (Jones and Moberg 2003) in an off-line mode. Therefore, a portion of the surface warming trend associated with regional characteristics above the surface (land cover types) may be reflected in the ERA40, resulting in a smaller OMR trend than that derived from NNR (Simmons et al. 2004; Lim et al. 2005) (Figs. 1e-h), although ERA40 could also contain bias passed from the in-situ surface measurements. From Figure 1 we conclude that both reanalyses could serve as a dataset for surface temperature trend analysis because they do not use the surface temperature observations directly, but for the purpose of assessing the surface temperature trend associated with surface vegetation characteristics, the NNR has the advantage of not using surface observations to initialize the soil temperature and moisture.

4. The OMR trends associated with surface vegetation

4.1. Geographical surface vegetation field and its annual range

Figure 2 represents the geographical distribution of the NDVI for the a) all 12 months, b) June-July-August (JJA), c) December-January-February (DJF), and d) the seasonal difference (JJA-DJF). The maps depict the pattern of global greenness, along with their annual ranges. The well-known desert areas such as Sahara, Middle East, western China, and Mongolia are classified into the least vegetated region (Figs. 2a-c). These areas show little seasonal vegetation change (Fig. 2d). Arctic areas are also characterized by small NDVI in summer and negative NDVI (frozen water) in winter. On the other hand, tropical evergreen forest regions including the equatorial Africa, southeast Asia and the Maritime Continent, central America, and Amazon areas show a large vegetation index with little seasonal change (Figs. 2a-c). Note that there are several grids over India and Indochina peninsula where the wintertime NDVI is greater than that in summer. This is because seasonal vegetation growth is a few months out of phase with monsoon precipitation over those regions. Monthly NDVI fields (not shown here) reveal that the leaf area index in the Indian region has its minima in the pre-monsoon season (April, May) and begins to increase slowly with the onset of the Indian summer monsoon. The summer monsoon gets to central India only by mid-June, and the period prior to that is very stressful for vegetation given the scorching heat and dryness of the pre-monsoon period. Rainfall in June/July is a relief, and vegetation begins to come back, reaching the largest NDVI values in

the post-monsoon season. The main crop cycle, wheat, called “rabi crops” begins with planting in fall and is nurtured by the milder winter monsoon rainfall; harvesting occurs in spring. Therefore, although initially surprising, the slightly higher NDVI in winter than in summer observed over India is representative of the actual vegetation characteristics. We have found that the same spatial NDVI features are reproduced in the other NDVI dataset derived from GIMMS (http://gimms.gsfc.nasa.gov/) group (Tucker et al. 2005).

Mid-latitude regions which generally comprise cropland, mixed (broad-leaf and needle-leaf) forests, shrub land, grass, and needle-leaf tree forests, have a much more conspicuous seasonal change (Figs. 2b-d). In those regions the large vegetation index in JJA period drops drastically during DJF period. While the seasonal vegetation change is strong in the European countries and North American region, the mid-latitude central Asia (Russia, northern China, and Mongolia) shows a relatively weak seasonal NDVI change due to the annually consistent aridity (e.g., Gobi desert) over the region (Fig. 2d).

4.2. Relationship between the OMR trend and the vegetation index

We now relate the surface temperature change signals estimated by OMR to the different surface vegetation indexes. To this end, the decadal OMR trend at each grid is scatter-plotted as a function of annual mean NDVI (Bounoua et al. 2000). This sort of approach is also found in Hanamean et al. (2003) in relating NDVI to 850-700mb layer mean temperature change derived from the NNR for the Colorado area.

As in Kalnay and Cai (2003), the OMR trend per decade at each grid point is obtained by taking the average of two decadal mean differences, that is, 90's – 80's and 70's – 60's, to avoid the small jumps in the reanalysis associated with the major addition of satellite observations in 1979. The decadal observation, reanalysis, and OMR trends are scatter-plotted with the NDVI values for the 20°S-50°N latitudinal band and all longitudes, an area where most of land mass is found (Hurrell and Trenberth 1998). NH high-latitudes including the arctic zone are not included in this analysis due to its different climate response mechanism to surface vegetation (Robock 1983; Wang and Key 2005) compared with mid- and low-latitude regions. Analysis of high-latitude regions is not within the scope of this study and will be investigated later.

As shown in Fig. 3a, decadal trends in GHCN observations show no significant relationship with the NDVI (r=-0.07), presumably because they reflect all climate change signals. However, the trend in NNR reanalysis (Fig. 3d) is significantly proportional to the vegetation index (r=0.56), indicating that it is missing the relationship demonstrated in modeling experiments (Xue and Shukla 1993; Dai et al. 2004; Hales et al. 2004) showing stronger surface warming in arid areas with low vegetation. This lack of reproduction of the surface temperature change signal associated with the impact of vegetation types is also present to a lesser extent in ERA40 reanalysis (r=0.17), as shown in Fig. 3b. Partial inclusion of surface information in ERA40 makes the correlation with NDVI less positive than NNR. The outliers in the scatter plots, i.e., large negative ERA40 trends and large NDVI, were all in the tropics, within 20^{o} latitude (Fig.

3b), whereas none of such an outliers were found for NNR (Fig. 3d).

Due to these characteristics of reanalysis data, the decadal OMR trend obtained from GHCN – ERA40 and GHCN – NNR, respectively, is negatively correlated with the surface vegetation index (r=-0.32, r=-0.67), demonstrating that the strong (weak) surface warming response to the surface aridity (greenness) is adequately represented by OMR, especially for "observation minus NNR". As shown in Figs. 3c and 3e, the inverse proportionality of decadal OMR trend to vegetation index is clearer for GHCN – NNR than GHCN – ERA40 because the former better extracts the surface temperature change signal associated with vegetation types.

Figure 4 is same as Fig. 3 but with the CRU instead of the GHCN observations. The key features in Fig. 4 are identical to those delineated in Fig. 3. While CRU observation trends are not correlated with the NDVI (r=0.11), the OMR trends have strong negative correlation with surface greenness, especially for CRU – NNR (r=-0.58).

4.3. Surface temperature change as a function of vegetation index

Decadal OMR trends with respect to the surface vegetation index are assessed. Figure 5 depicts the annual mean OMR trends as a function of NDVI values with 0.1 intervals. The OMR trend values at each grid point are averaged for the same surface vegetation index values. Trend values are represented by closed circles, along with the error range at 95% significance level by cross marks. The number of stations used for calculation of these trends is given in Table 1.

The two independent reanalyses appear to have a very similar dependence of the OMR trends with respect to surface vegetation as well as their statistical significance levels. The key features in the OMR trends for the 20°S~50°N latitudes ((i)~(iv)) are:

(i) The OMR trend decreases with the surface vegetation index. The quantitative estimate from the NNR reanalysis reveals that for vegetation index greater than 0.4 there is near zero additional near surface contribution to temperature change (Figs. 5a, b). Error ranges at 95% significance level support the statistical confidence of this assessment. The highest vegetation index area generally comprises the broadleaf forest over tropical forest regions. As discussed in modeling works by Shukla et al. (1990), Xue and Shukla (1993), and Giambelluca et al. (1997), this area is characterized by the strong transpiration and evaporative cooling feedback from the leaves, resulting in the suppression of surface warming.

(ii) The OMR trends over the moderate surface vegetation index (0.2~0.4) area are in the range of 0.1~0.2°C/decade (CRU-NNR, and GHCN-NNR) (Figs. 5a, b). These areas are mainly composed of mid-latitudinal crop and grass land, deciduous broadleaf or needleaf trees, and shrubs. Because they are less green than the tropical forest areas, the cooling feedbacks from leaves are weaker than those in tropical forest areas. This contributes to the moderation of surface warming over these areas.

(iii) Areas of less than 0.1 greenness with sparse vegetation show the largest warming associated with surface effects, ~0.3°C/decade (CRU-NNR, and GHCN-

NNR) (Figs. 5a, b). Areas where soil moisture is very limited and the land surface is characterized by bare soil, the evaporation negative feedback would be negligible, explaining a larger regional surface warming response under the same amount of radiative forcings, as discussed in Shukla et al. (1990), Bounoua et al. (2000), Hoffmann and Jackson (2000), Dai et al. (2004), Hales et al. (2004), Diffenbaugh (2005), and Saito et al. (2006).

(iv) The OMR trends for the ERA40 reanalysis (Figs. 5c,d) are similar but less pronounced than the trends for the NNR due to the partial inclusion of the surface processes associated with land vegetation types in the ERA40 which are not included in the NNR.

5. Surface temperature trend response to the seasonal vegetation change

5.1. Monthly variation of correlation between OMR trend and vegetation

As shown in Fig. 2, the vegetation index has a seasonal variation, especially for mid-latitudes. The spatial correlations between the NDVI and the OMR trend for each month is now calculated to understand the seasonal variation of OMR trends associated with seasonal vegetation changes. Since the NDVI shows seasonal changes at fixed location, we expect that the OMR trend would also exhibit a temporal variation in response to the seasonal vegetation change. Month-to-month variation of correlations between the NDVI and the OMR trend identifies that they range from -0.6 to -0.35 (Fig. 6 (lines with cross mark)). The observed negative correlations indicate that the OMR trend satisfies the negative relationship with the NDVI throughout the year, i.e., there is an increase

(decrease) in OMR trend with decreasing (increasing) vegetation. Seasonal difference in the OMR trend also indicates that the trend is more negatively correlated with NDVI when the overall vegetation is low (in the winter) than when it is high (the summer). On the other hand, the observed decadal trends (GHCN and CRU) show weak correlations with NDVI seasonal variations (less than 0.2), indicating little significant relationship with surface vegetation types throughout the year, because, as observed before, the observed trends are dominated by combined atmospheric and surface warming effects, not only by vegetation effects (Fig. 6, lines with open circles).

5.2. Variation of the OMR trend with the seasonal vegetation change

Based on the understanding that the OMR trend varies with the temporal vegetation change, the seasonal variation of the OMR trends is estimated for several major regions over the NH. Five different regions are chosen here to investigate the response of the OMR trends for the NNR to the variation of the surface vegetation. In Figure 7 we consider two extremes with low amplitude in the NDVI seasonal cycle. First, desert areas (Sahel and Middle-East) are selected as areas of little vegetation, limited soil moisture, and little seasonal vegetation change. Second, low-latitude broadleaf forests (equatorial Africa, Amazon, Indochina peninsula and Maritime Continent) are chosen as representative of high vegetation, abundant soil moisture, and ever-greenness. In Figure 8, by contrast, we select areas of strong seasonal vegetation change between summer and winter in mid-latitudes, e.g., Europe and USA, and the arid mid-latitude central Asia.

The seasonal variation of the OMR trend for NNR clearly shows that strong surface warming (~0.4°C/decade) beyond what would be expected from atmospheric warming is observed over the desert area throughout the year (see red solid lines in Fig. 7a) as the NDVI remains close to zero (black solid line). Limited soil-moisture and little evaporative cooling feedback all year round appear to drive the consistent strong warming over this area (Dai et al. 2004; Hales et al. 2004).

In contrast, tropical evergreen forest area in Fig. 7b shows little surface warming throughout the year (red solid line) due to the ever-greenness (black solid line). Surface cooling by evaporation, transpiration, and soil moisture associated with surface greenness and tropical humid climate remains effective throughout the year, yielding little surface warming in every month (Xue and Shukla 1993).

In mid-latitudes such as Europe (Fig. 8a) and USA (Fig. 8b), OMR trends exhibit a strong annual cycle as the NDVI has strong seasonal changes (black solid line), with high vegetation in the summer and low vegetation in the winter. The corresponding OMR trend fluctuates seasonally almost out of phase with the seasonal NDVI oscillation. Therefore, we can conclude that the surface warming response to the regional vegetation status over the mid-latitude tends to be strong in winter and early spring (0.2~0.3°C/decade) when the vegetation is low but weak in summer and early fall (0.1°C/decade) with high vegetation.

The OMR trend over the mid-latitude central Asia (Russia, northern China, and Mongolia) does not show a strong seasonal variation, as shown in Fig. 8c.

As seen in the NDVI (black line), this area is characterized by being arid throughout the year. Therefore, the OMR trend remains high with little seasonal change despite being in a mid-latitude geographical location.

We clearly demonstrated how sensitively the OMR trend for NNR responds to the seasonal vegetation change. However, the variation of OMR trend for ERA40 does not show any significant relationship with the seasonal vegetation change in Fig. 7 and 8 (see blue solid line). As discussed before, the partial inclusion of surface temperature information in the ERA40 makes the OMR temperature change signal associated with seasonal vegetation change weaker.

6. Summary and discussions

Anomalies in monthly surface temperature time series derived from two reanalyses (NNR and ERA40) and two observational datasets (GHCN and CRU) are analyzed by OMR approach (observation minus reanalysis) to 1) investigate the relationship between the OMR trend and land vegetation types and 2) assess the surface temperature change signal by the impact of independent land vegetation types from the OMR. The rationale for the OMR approach is that while reanalyses contain the large-scale temperature change signals that could be forced by greenhouse gases, volcanoes, and natural decadal variability, the NNR and (to a lesser extent) the ERA40 are insensitive to regional surface processes associated with different land vegetation types because little surface data or information were used in the data assimilation process. Pronounced features identified from analysis are:

1) The long-term trends for both observations and reanalyses averaged over several areas show a gradual warming, with greater upward trend in observations over the last 4 decades. This is caused by the poor reproduction of surface temperature change signal associated with impacts of regional vegetation types in the reanalyses data. As a result, the difference time series between observation and reanalyses (observation minus reanalysis, OMR) grows with time.

2) The positive OMR trend is larger for NNR than for ERA40 due to the different data assimilations used in the two reanalyses. The NNR used no surface observations over land, whereas ERA40 used surface temperature observations to initialize soil temperature and moisture. This makes the NNR reanalysis more insensitive to surface processes than the ERA40. As a result of this lack of surface information in the NNR, more surface temperature change signal resulting from the impact of different land vegetation types are captured in the OMR time series using NNR than ERA40 (Kalnay and Cai 2003; Zhou et al. 2004; Fraunfeld et al. 2005; Lim et al. 2005). This fact gives an indication that the OMR time series for NNR would provide useful information to assess the multi-decadal surface temperature change signal with regard to different land vegetation types. Nevertheless, the general dependence of OMR on vegetation type is clearly similar between the two reanalyses.

3) For a clearer demonstration of the relationship, the decadal OMR trends at each grid were correlated with NDVI. The results prove that the decadal OMR trend is inversely proportional to NDVI with statistical significance (correlation < -0.5). The OMR trend for the NNR yields a more negative correlation with NDVI

(corr. = -0.58 (CRU – NNR) and -0.67 (GHCN – NNR)) than the OMR trend for the ERA40 does (corr. = -0.26 (CRU – ERA40) and corr.=-0.32 (GHCN – ERA40)). This suggests that the decadal trend of the "observation – NNR" substantially account for the impact on surface warming effects associated with different land vegetation types, absent in the NNR.

This feature is robust with respect to seasonal changes in the NDVI. Correlations range from -0.6 to -0.35 throughout the year, indicating that for the NNR the decadal OMR trend varies with seasonal NDVI change at fixed locations to maintain the negative correlation.

4) The surface temperature change signal inferred from the OMR trend is also assessed as a function of surface vegetation index. It shows that the trend is very sensitive to the different surface greenness. The strongest warming trend due to surface processes is found over the desert areas (Sahara, Middle East, western China (Tibet) and Mongolia) (~0.3-0.4°C/decade) whereas tropical forest areas (equatorial Africa, southeast Asia, Maritime Continent, and Amazon), are associated with negligible warming or slight cooling (~0°C/decade). These results are consistent with Dai et al. (2004), Hales et al. (2004), and Diffenbaugh (2005), who argue that there is stronger (weaker) warming in barren (vegetated) areas due to the response of surface albedo, soil moisture, and evaporative cooling feedback to solar radiative forcing. Several mid-latitude areas where the vegetation density lies in between desert and tropical forest show a moderate decadal warming (~0.2°C/decade).

5) The OMR trend patterns are strongly dependent on seasonal vegetation

change for mid-latitudes areas such as Europe and North America, where the strong seasonal vegetation takes place show weak warming trend (~0.1°C/decade) in summer and early fall whereas strong warming (0.2~0.3°C/decade) in winter and early spring. This is in agreement with the studies of Shukla et al. (1990) and Xue and Shukla (1993) who have shown that vegetation changes by forestation (deforestation) suppresses (enhances) the surface warming effect.

In contrast, tropical forest areas and desert areas (Sahara and Middle East) tend to show a constant OMR trend throughout the year, as their regions exert little vegetation change with season. Despite of the geographical mid-latitude location, the OMR trend in the central Asia region remains high without any noticeable seasonal change due to the stationary aridity throughout the year.

The findings obtained in this study support our argument that the surface temperature change signal associated with different land vegetation types are reasonably well captured by the OMR approach. The analysis demonstrates that lower long-term trends in the reanalysis surface temperature than observations are attributable to the absence in surface data in the data assimilation procedure. As a result, the OMR approach facilitates isolating the impact of vegetation types on long-term surface temperature trend by removing large-scale global warming signal as recorded in the reanalysis from the surface observation.

These findings could be affected by other errors that might arise from the reanalysis inhomogeneity in time, from model systematic errors and observation biases. Our OMR analysis tried to minimize the impact of those errors by 1) averaging the trends for relatively homogeneous reanalysis periods, 2) calculating

the trends for the anomalies with respect to a 30-year annual cycle, and 3) choosing the most reliable observation data currently being used. The clear relationship between the OMR trend and NDVI suggests that the effect of these errors is relatively small compared to the temperature change signal that we tried to isolate.

It should be also noted that the NDVI is applied under the assumption that the global distribution of the surface vegetation for each calendar month is approximately constant. The real NDVI time series for each calendar month exhibit some interannual variation (not shown), but the amplitude of the changes is small, especially on a decadal scale. We believe that this assumption is reasonable since there have been no large interannual NDVI changes (e.g., a switch between forest and desertic bare soil) on a 5°×5° horizontal grid scale that would be needed to have a noticeable effect on the OMR trend values.

7. Acknowledgement

This study was supported by the National Science Foundation (ATM-0403211 and ATM-0403518) and by the Climate Change Data and Detection program of NOAA Office of Global Programs (GC04-259). ERA40 data were obtained from the ECMWF public web server, http://data.ecmwf.int/data. We thank three anonymous reviewers for very helpful and constructive comments. We also express our gratitude to Profs. S. Nigam, J. Shukla, J. Srinivasan and S. Gadgil for their insightful comments on why the NDVI seems to be out of phase with precipitation in India.

References

Betts, A. K., J. H. Ball, and P. Viterbo, 2003: Evaluation of the ERA-40 surface water budget and surface temperature for the Mackenzie river basin. *J. Hydrometeor.*, **4**, 1194-1211.

Bounoua, L., G. J. Collatz, S. O. Los, P. J. Sellers, D. A. Dazlich, C. J. Tucker, and D. A. Randall, 2000: Sensitivity of climate to changes in NDVI. *J. Climate*, **13**, 2277-2292.

Cai, M., and E. Kalnay, 2004: Impact of land-use change on climate: Response to the comments by Rose et al. and Trenberth. *Nature*, **427**, 214-214.

Cai, M., and. E. Kalnay, 2005: Can reanalysis have anthropogenic climate trends without model forcing? *J. Climate*, **18**, 1844-1849.

Chelliah, M., and C. F. Ropelewski, 2000: Reanalysis-based tropospheric temperature estimates: Uncertainties in the context of global climate change detection. *J. Climate*, **13**, 3187-3205.

Dai, A, K. E. Trenberth, and T. Qian, 2004: A global dataset of Palmer drought severity index for 1870-2002: Relationship with soil moisture and effects of surface warming. *J. Hydrometeor.*, ***5***, 1117-1130.

Diffenbaugh, N. S., 2005: Atmosphere-land cover feedbacks alter the response of surface temperature to CO_2 forcing in the western United States. *Clim. Dyn.*, **24**, 237-251.

Easterling, D. R., T. C. Peterson, and T. R. Karl, 1996: On the development and use of homogenized climate datasets. *J. Climate*, **9**, 2941-2944.

Frauenfeld, O. W., T. Zhang, and M. C. Serreze, 2005: Climate change and variability

using European Center for Medium-Range Weather Forecast analysis (ERA-40) temperatures on the Tibetan Plateau. *J. Geophys. Res.,* **110**, D02101, doi:10.1029/2004JD005230.

Giambelluca, T. W., D. Hölscher, T. X. Bastos, R. R. Frazão, M. A. Nullet, and A. D. Ziegler, 1997: Observations of albedo and radiation balance over postforest land surfaces in the eastern Amazon basin. *J. Climate*, **10**, 919-928.

Hales, K., J. D. Neelin, and N. Zeng, 2004: Sensitivity of tropical land climate to leaf area index: Role of surface conductance versus albedo. *J. Climate*, **17**, 1459-1473.

Hanamean, J. R., R. A. Pielke, C. L. Castro, D. S. Ojima, B. C. Reed, and Z. Gao, 2003: Vegetation greenness impacts on maximum and minimum temperatures in northeast Colorado. *Meteor. Applications*, **10**, 203-215.

Hansen, J. E., R. Ruedy, M. Sato, M. Imhoff, W. Lawrence, D. Easterling, T. Peterson, and T. Karl, 2001: A closer look at United States and global surface temperature change. *J. Geophys. Res*., **106**, 23947-23963.

Hegerl, G. C., and J. M. Wallace, 2002: Influence of patterns of climate variability on the difference between satellite and surface temperature trends. *J. Climate*, **15**, 2412-2428.

Hoffmann, W. A., and R. B. Jackson, 2000: Vegetation-climate feedbacks in the conversion of tropical savanna to grassland. *J. Climate*, **13**, 1593-1602.

Hurrell, J. W., and K. E. Trenberth, 1998: Difficulties in obtaining reliable temperature trends: Reconciling the surface and satellite microwave sounding unit records. *J.*

Climate, **11**, 945-967.

IPCC, 2001: *Climate Change 2001: The scientific basis*, Cambridge University Press.

James, M. E., and S. N. Kalluri, 1994: The Pathfinder AVHRR land data set: an improved coarse-resolution data set for terrestrial monitoring. *Int. J. Rem. Sen*., **15**, 3347-3363.

Jones, P. D., and A. Moberg, 2003: Hemispheric and large-scale surface air temperature variations: An extensive revision and an update to 2001. *J. Climate,* **16**, 206-223.

Kabat, P., M. Claussen, P. A. Dirmeyer, J. H. C. Gash, L. Bravo de Guenni, M. Meybeck, R. A. Pielke Sr., C. J. Vorosmarty, R. W. A. Hutjes, and S. Lutkemeier, Editors, 2004: Vegetation, water, humans and the climate: A new perspective on an interactive system. Springer, Berlin, Global change – The IGBP series, 566 pp.

Kalnay, E., and Coauthors, 1996: The NCEP/NCAR 40-year reanalysis project. *Bull. Amer. Meteor. Soc.*, **77**, 437-471.

Kalnay, E., and M. Cai, 2003: Impact of urbanization and land-use on climate change. *Nature*, **423**, 528-531.

Kalnay, E., M. Cai, H. Li, and J. Tobin, 2006: Estimation of the impact of land-surface forcings on temperature trends in eastern Unites States. *J. Geophys. Res*., 111, D06106,doi:10.1029/2005JD006555.

Kistler, R., and Coauthors, 2001: The NCEP/NCAR 50-year reanalysis: monthly means CD-ROM and documentation. *Bull. Amer. Meteor. Soc*., **82**, 247-267.

Lim, Y.-K., M. Cai, E. Kalnay, and L. Zhou, 2005: Observational evidence of sensitivity

of surface climate changes to land types and urbanization. *Geophys. Res. Lett.*, **32**, L22712, doi:10.1029/2005GL024267.

Palmer, T. N., C. Brankovic, F. Molteni, S. Tibaldi, L. Ferranti, A. Hollingsworth, U. Cubasch, and E. Klinker, 1990: The European center for medium-range weather forecasts (ECMWF) program on extended-range prediction. *Bull. Amer. Meteor. Soc.*, **71**, 1317-1330.

Pepin, N. C., M. Losleben, M. Hartman, and K. Chowanski, 2005: A comparison of SNOTEL and GHCN/CRU surface temperatures with free-air temperatures at high elevations in the western United States: Data compatibility and trends. *J. Climate*, **18**, 1967-1985.

Peterson, T. C., and R. S. Vose, 1997: An overview of the Global Historical Climatology Network temperature database. *Bull. Amer. Meteor. Soc*., **78**, 2837-2848.

Pielke Sr, R. A., and Coauthors, 2002: The influence of land-use change and landscape dynamics on the climate system: relevance to climate-change policy beyond the radiative effects of greenhouse gases. *Phil. Trans. Roy. Soc. Lond*, **360**, 1705-1719.

Robock, A., 1983: Ice and snow feedbacks and the latitudinal and seasonal distribution of climate sensitivity. *J. Atmos. Sci*., **40**, 986-997.

Saito, K., T. Yasunari, and K. Takata, 2006: Relative roles of large-scale orography and land surface processes in the global hydroclimate. Part II: impacts on hydroclimate over Eurasia. *J. Hydrometeor.*, **7**, 642-659.

Sellers, P. J., 1985: Canopy reflectance, photosynthesis and transpiration. *Int. J.*

Remote Sens., **6**, 1335-1372.

Shukla, J., C. Nobre, and P. Sellers, 1990: Amazon deforestation and climate change. *Science*, **247**, 1322-1325.

Simmons, A. J., and Coauthors, 2004: Comparison of trends and low-frequency variability in CRU, ERA-40, and NCEP/NCAR analyses of surface air temperature. *J. Geophys, Res*., **109**, D24115, doi:10.1029/2004JD005306.

Trenberth, K. E., 2004: Climatology – Rural land-use change and climate. *Nature*, **427**, 213-213.

Tucker, C. J., J. E. Pinzon, M. E. Brown, D. A. Slayback, E. W. Pak, R. Mahoney, E. F. Vermote, and N. E. Saleous, 2005: An extended AVHRR 8-km NDVI dataset compatible with MODIS and SPOT vegetation NDVI data. *Int. J. Rem. Sen*., **26**, 4485-4498.

Vose, R. S., T. R. Karl, D. R. Easterling, C. N. Williams, and M. J. Menne, 2004: Climate – Impact of land-use change on climate. *Nature*, **427**, 213-214.

Wang, X., and J. R. Key, 2005: Arctic surface, cloud, radiation properties based on the AVHRR polar pathfinder dataset. Part II: recent trends. *J. Climate*, **18**, 2575-2593.

Xue, Y., and J. Shukla, 1993: The influence of land surface properties on Sahel climate. Part I: desertification. *J. Climate*, **6**, 2232-2245.

Zhou, L., R. E. Dickinson, Y. Tian, J. Fang, Q. Li, R. K. Kaufmann, C. J. Tucker, and R. B. Myneni, 2004: Evidence for a significant urbanization effect on climate in China. *Proceedings of the National Academy of Sciences,* **101**, 9540-9544.

Table caption

Table 1. The number of grid points used for calculation of OMR trends in Fig. 5.

	NDVI < 0.1	0.1 ≤ NDVI < 0.2	0.2 ≤ NDVI < 0.3	0.3 ≤ NDVI < 0.4	0.4 ≤ NDVI < 0.5	0.5 ≤ NDVI
GHCN-NNR	52	35	35	67	88	74
CRU-NNR	57	35	37	70	95	82
GHCN-ERA40	52	35	35	67	88	74
CRU-ERA40	57	35	37	70	95	82

Figure Captions

Figure 1. Time-series (ten year running mean) of the surface temperature anomalies (°C) averaged over the a) East Asia, b) Europe & West Asia, c) North & South America, and d) Africa area. Anomaly values are obtained by removing the 30-yr mean from 1961 to 1990 and they are further adjusted to have zero mean over the last 10 years (1993-2002). Right panels are same as figures in the left panel but for their OMR (CRU – ERA40, CRU – NNR, GHCN – ERA40, and GHCN – NNR) time series.

Figure 2. Surface vegetation map derived from NDVI. Vegetation index are averaged over a) 1981 – 1994, b) summer (JJA), and c) winter (DJF). The seasonal NDVI difference (JJA-DJF) is shown in (d).

Figure 3. Scatter diagram between the NDVI and the decadal surface temperature trend of a) GHCN, b) ERA40, c) GHCN – ERA40, d) NNR, and e) GHCN – NNR over (0°-360°E)×(20°S-50°N) region. Data have been spatially smoothed to remove the extreme outliers. Abscissa denotes the NDVI whereas the ordinate the decadal trend. Here *r* is the correlation coefficient of all the data points.

Figure 4. Same as Fig. 3 but for a) CRU, c) CRU – ERA40, and e) CRU – NNR.

Figure 5. Assessment of annual mean OMR trend (°C/decade) (lines with filled circles) as a function of annual mean NDVI. The top panels denote the OMR trend for NNR reanalysis whereas the bottom panels for ERA40 reanalysis. Lines with cross mark represent the error range at 95% significance level. Abscissa and ordinate represent the NDVI and the OMR trend, respectively.

Figure 6. Month-to-month variation of the correlation between NDVI and the decadal

OMR trend over (0°-360°E)×(20°S-50°N) region. The trend values have been temporally smoothed by 5-month running mean to remove the extreme outliers. Lines with open circle denote the CRU (long-dash) and the GHCN (solid) whereas cross the CRU – NNR (long-dash) and GHCN – NNR (solid). Abscissa and ordinate denote the time in months and the correlation coefficient, respectively.

Figure 7. Seasonal variation of the OMR trend in response to the seasonal vegetation change over a) Desertic area (Sahara & Middle East) and b) Tropical evergreen forest (Equatorial Africa and Asia, and Amazon). Red lines with closed circle and closed square, respectively, denote the seasonal variation of OMR trend of "GHCN – NNR" and "CRU – NNR". Blue lines are plotted by switching NNR to ERA40 reanalysis. Seasonal NDVI change is denoted by black solid line. Abscissa denotes the time in months whereas the ordinate the decadal trend in °C/decade (for red and blue lines) and the NDVI value (for black line).

Figure 8. Same as Fig. 7 but for the mid-latitude land-mass, a) Europe, b) USA, and c) central Asia with aridity covering Russia, northern China, and Mongolia.

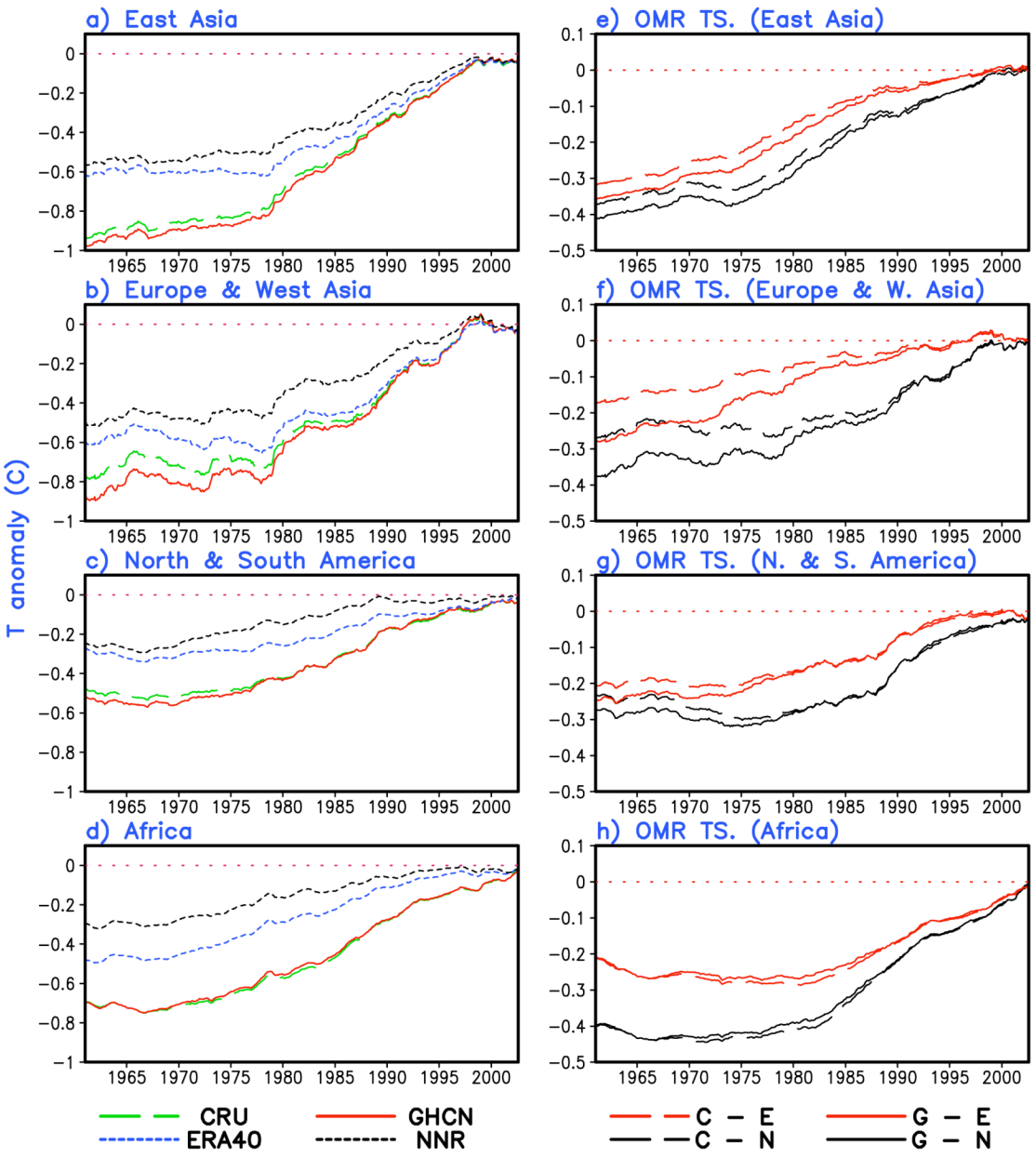

Figure 1. Time-series (ten year running mean) of the surface temperature anomalies (°C) averaged over the a) East Asia, b) Europe & West Asia, c) North & South America, and d) Africa area. Anomaly values are obtained by removing the 30-yr mean from 1961 to 1990 and they are further adjusted to have zero mean over the last 10 years (1993-2002). Right panels are same as figures in the left panel but for their OMR (CRU – ERA40, CRU – NNR, GHCN – ERA40, and GHCN – NNR) time series.

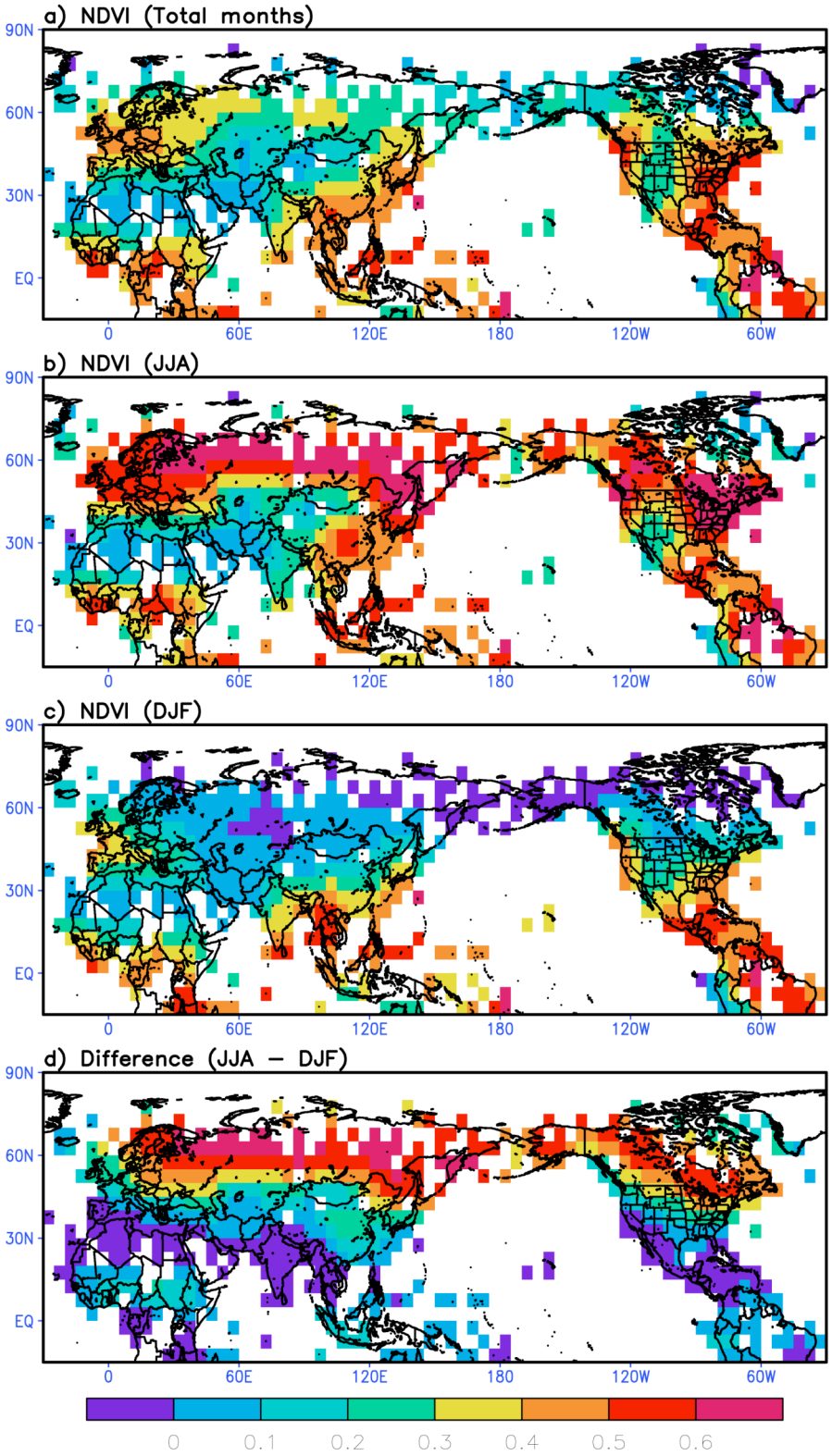

Figure 2. Surface vegetation map derived from NDVI. Vegetation index are averaged over a) 1981 – 1994, b) summer (JJA), and c) winter (DJF). The seasonal NDVI difference (JJA-DJF) is shown in (d).

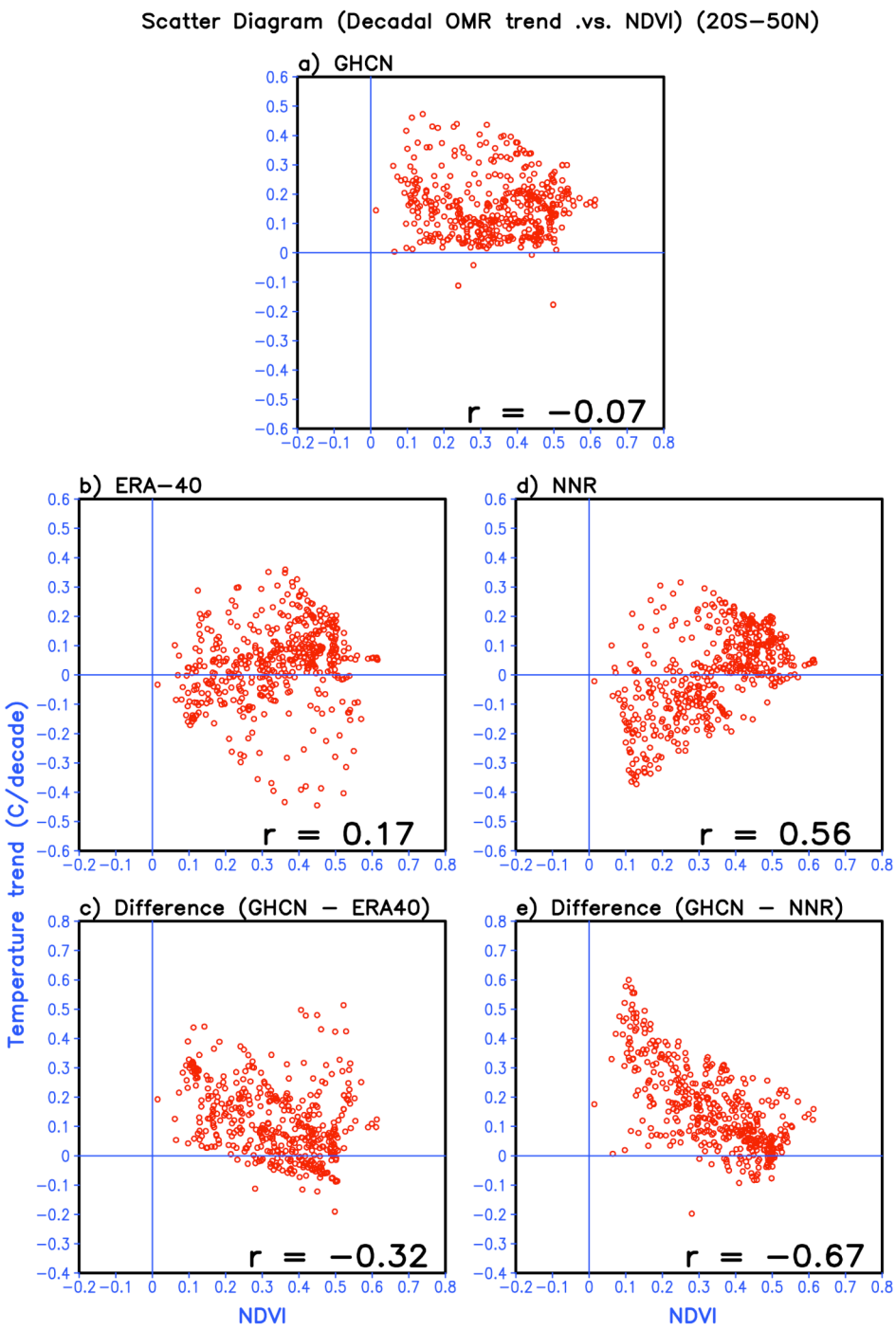

Figure 3. Scatter diagram between the NDVI and the decadal surface temperature trend of a) GHCN, b) ERA40, c) GHCN – ERA40, d) NNR, and e) GHCN – NNR over (0°-360°E)×(20°S-50°N) region. Data have been spatially smoothed to remove the extreme outliers. Abscissa denotes the NDVI whereas the ordinate the decadal trend. Here *r* is the correlation coefficient of all the data points.

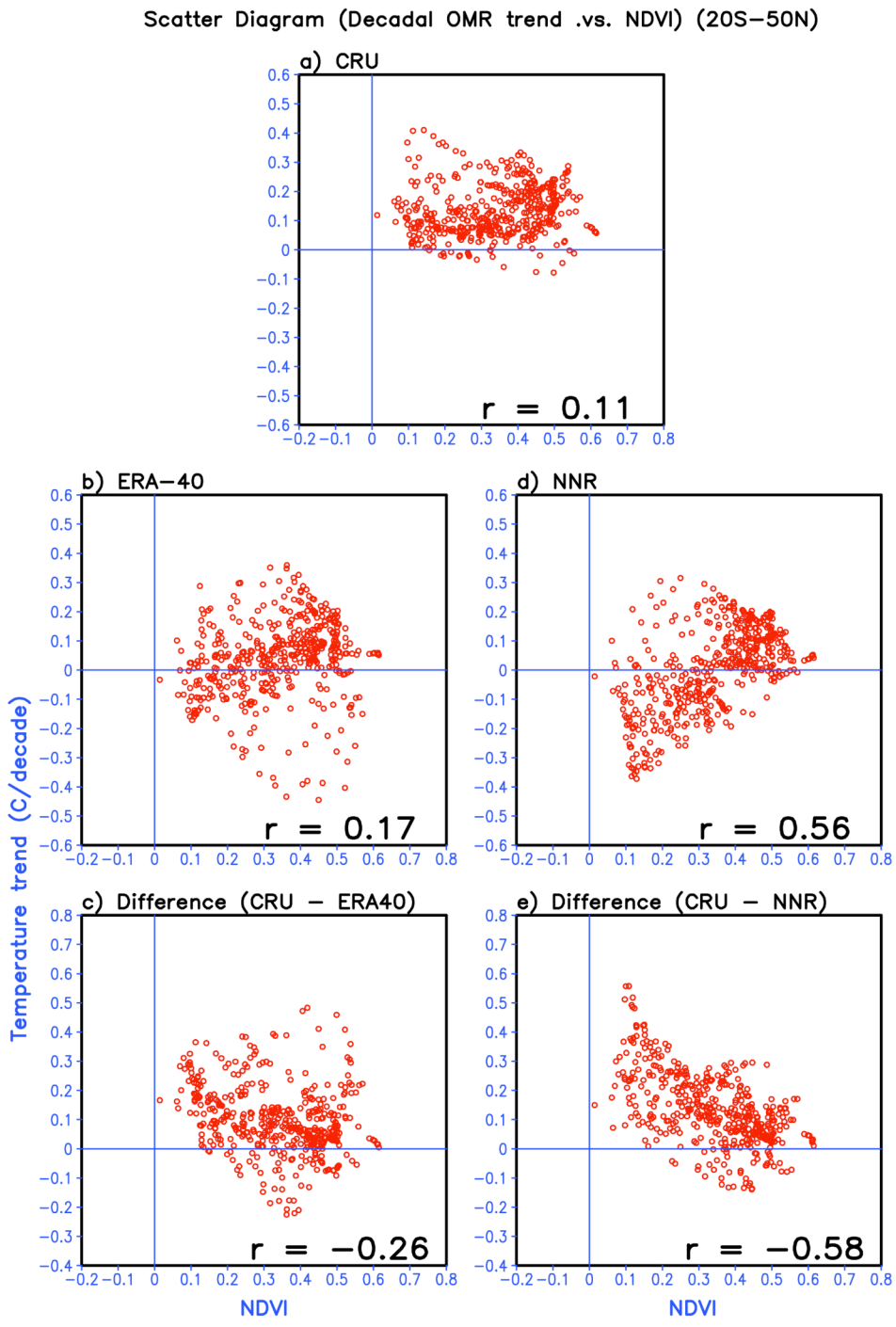

Figure 4. Same as Fig. 3 but for a) CRU, c) CRU – ERA40, and e) CRU – NNR.

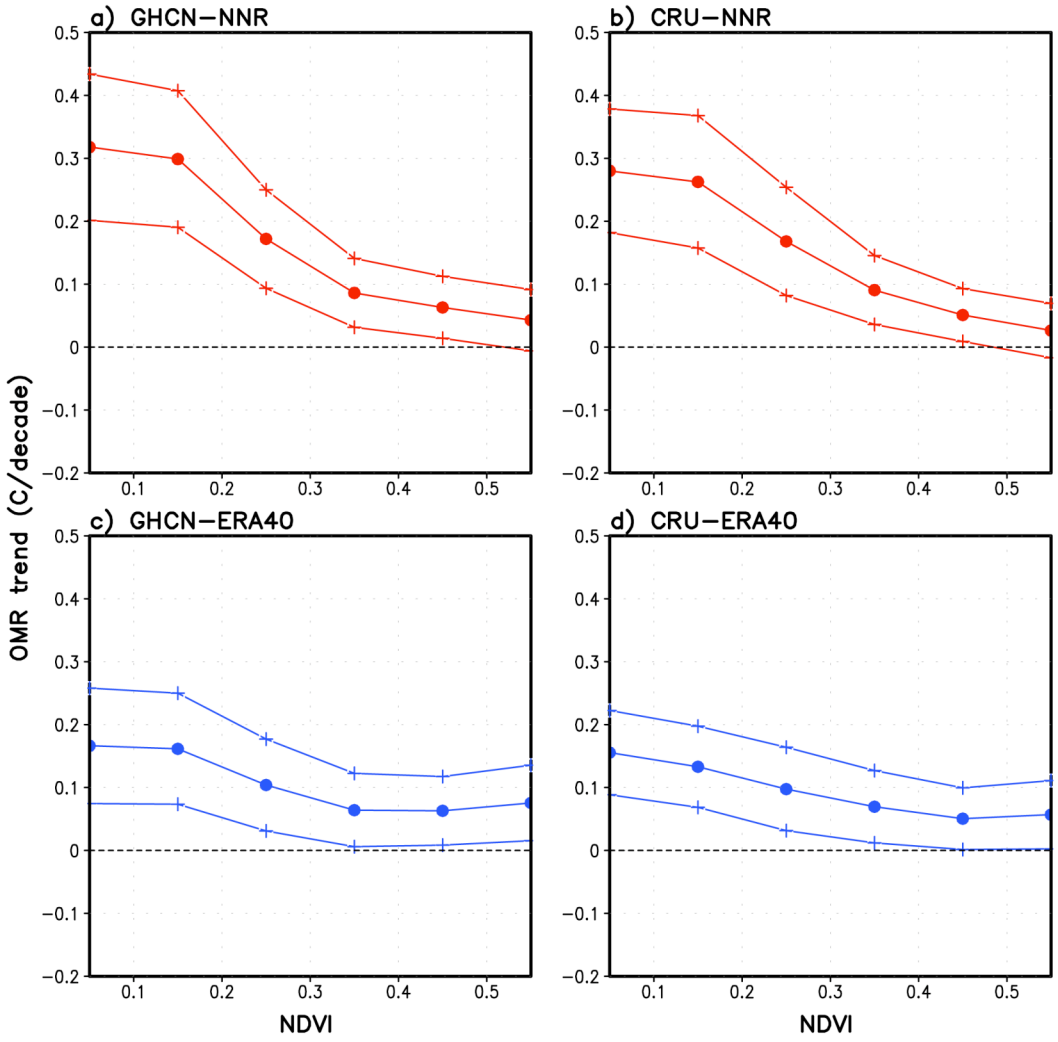

Figure 5. Assessment of annual mean OMR trend (°C/decade) (lines with filled circles) as a function of annual mean NDVI. The top panels denote the OMR trend for NNR reanalysis whereas the bottom panels for ERA40 reanalysis. Lines with cross mark represent the error range at 95% significance level. Abscissa and ordinate represent the NDVI and the OMR trend, respectively.

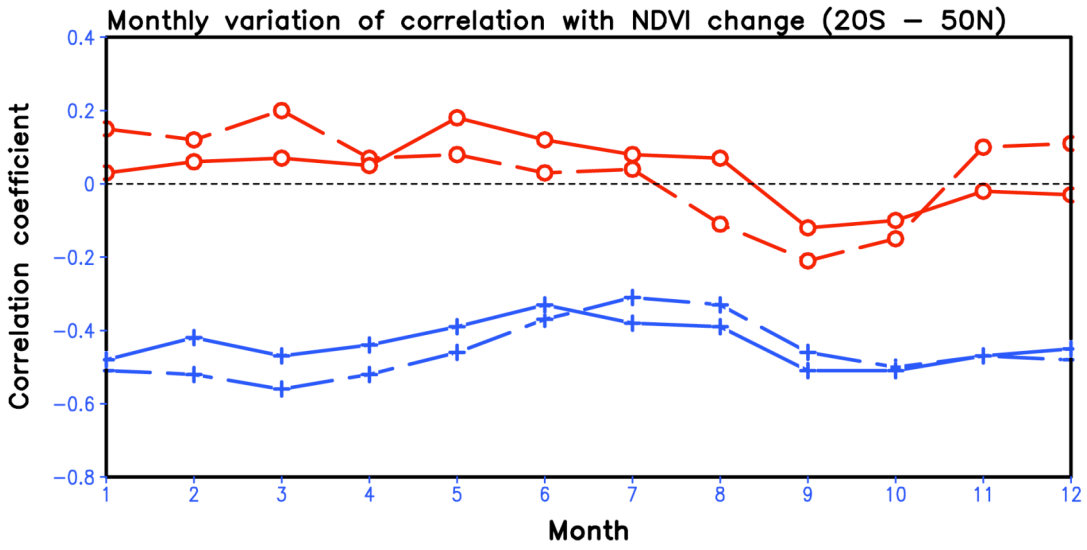

Figure 6. Month-to-month variation of the correlation between NDVI and the decadal OMR trend over (0°-360°E)×(20°S-50°N) region. The trend values have been temporally smoothed by 5-month running mean to remove the extreme outliers. Lines with open circle denote the CRU (long-dash) and the GHCN (solid) whereas cross the CRU – NNR (long-dash) and GHCN – NNR (solid). Abscissa and ordinate denote the time in months and the correlation coefficient, respectively.

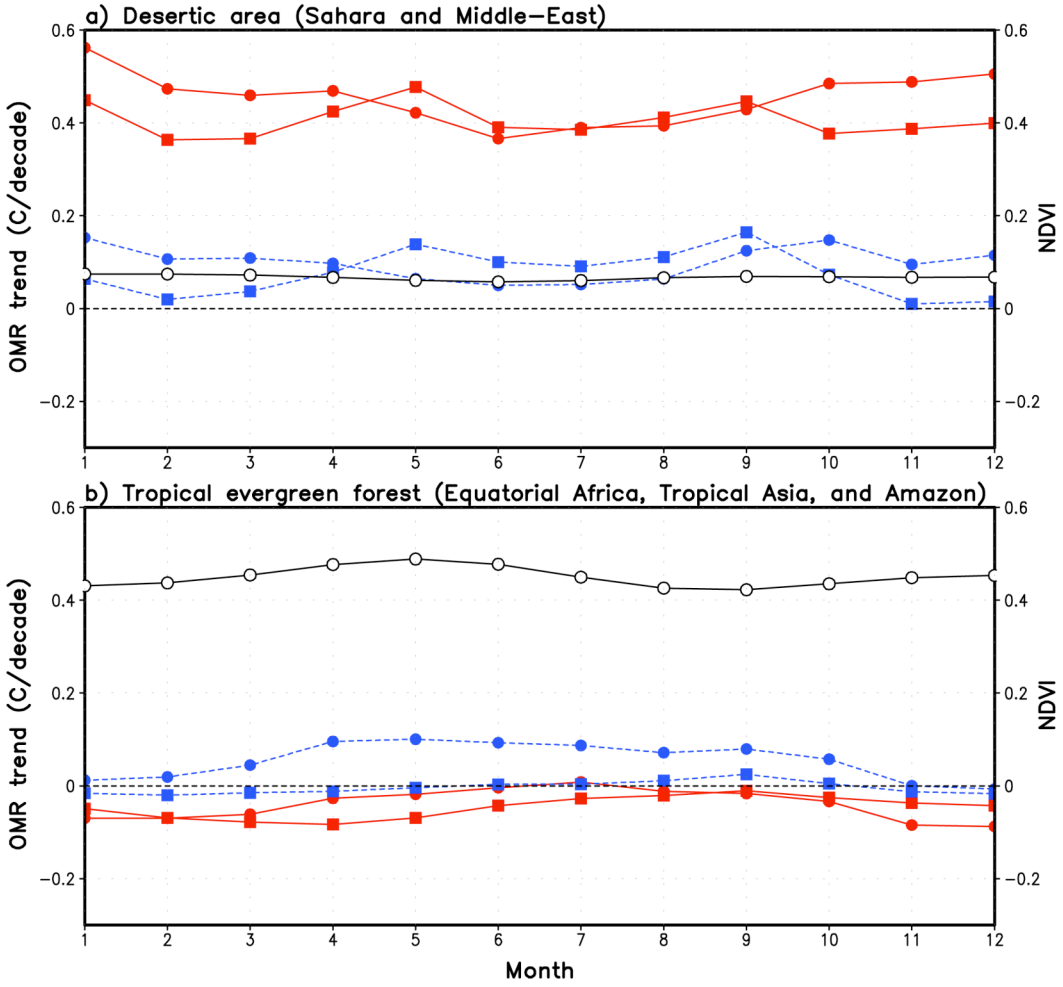

Figure 7. Seasonal variation of the OMR trend in response to the seasonal vegetation change over a) Desertic area (Sahara & Middle East) and b) Tropical evergreen forest (Equatorial Africa and Asia, and Amazon). Red lines with closed circle and closed square, respectively, denote the seasonal variation of OMR trend of "GHCN – NNR" and "CRU – NNR". Blue lines are plotted by switching NNR to ERA40 reanalysis. Seasonal NDVI change is denoted by black solid line. Abscissa denotes the time in months whereas the ordinate the decadal trend in °C/decade (for red and blue lines) and the NDVI value (for black line).

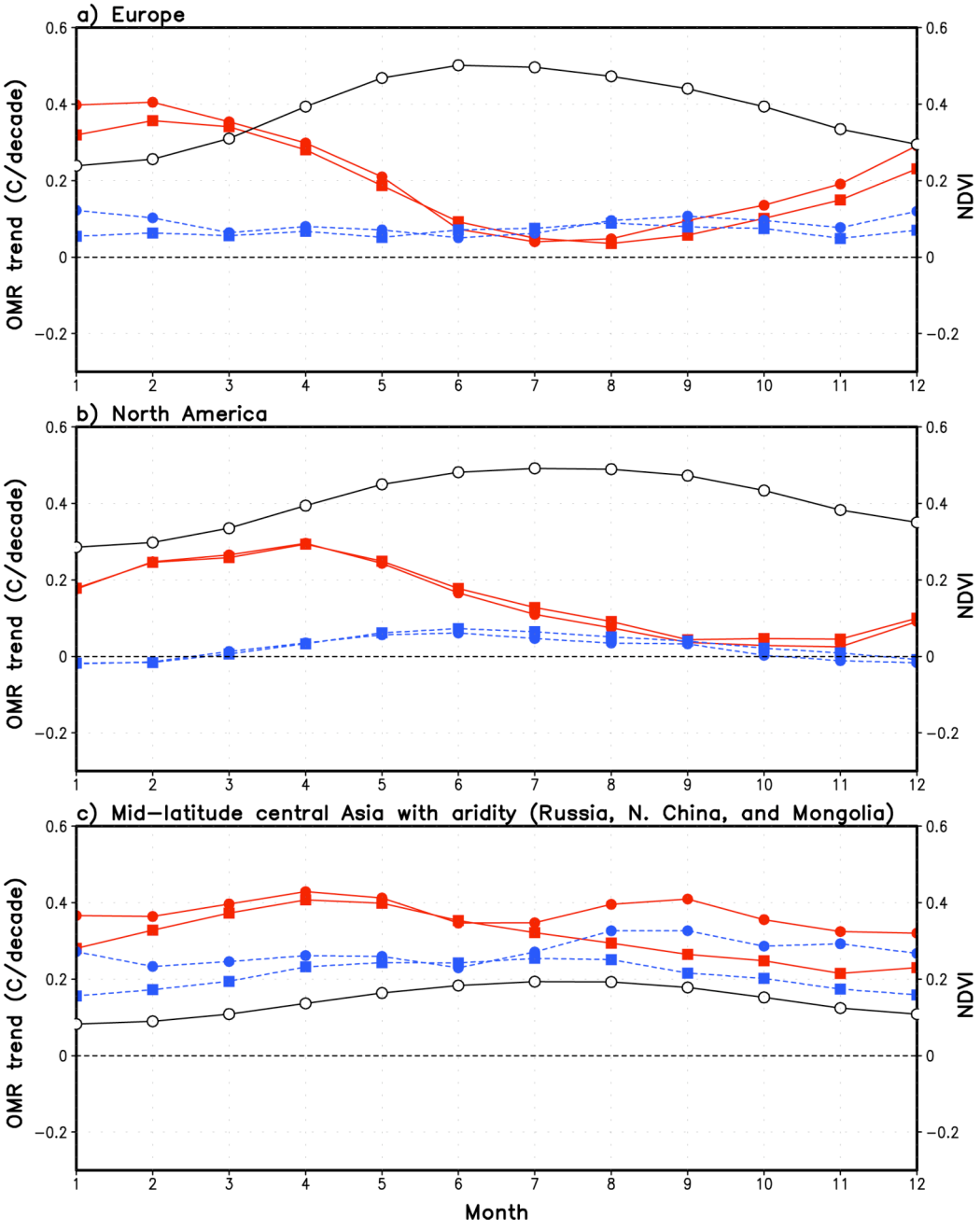

Figure 8. Same as Fig. 7 but for the mid-latitude land-mass, a) Europe, b) USA, and c) central Asia with aridity covering Russia, northern China, and Mongolia.